

Laser Induced Gas Vortices

Uri Steinitz*, Yehiam Prior & Ilya Sh. Averbukh

*Department of Chemical Physics, Weizmann Institute of Science, 234 Herzl Street, Rehovot, Israel 76100**

(Dated: October 30, 2018)

Properly polarized and correctly timed femtosecond laser pulses have been demonstrated to create rotational states with a preferred sense of rotation. We show that due to conservation of angular momentum, collisional relaxation of these unidirectionally rotating molecules leads to the generation of macroscopic vortex flows in the gas. The emerging velocity field converges to a self-similar Taylor vortex, and repeated laser excitations cause a continuous stirring of the gas.

PACS numbers: 33.80.-b, 37.10.Vz, 47.32.Ef

Nowadays, femtosecond lasers are routinely used to manipulate and control molecular rotation and orientation in space [1, 2]. Particularly, diverse techniques have been developed to bring gas molecules to a rapidly spinning state with a preferred sense of rotation. These schemes include the optical centrifuge [3–5] and the molecular propeller [6, 7] methods, excitation by a chiral pulse train [8] and other techniques that are currently discussed [9, 10]. In rarefied gas, coherent effects such as alignment revivals have been widely investigated. Most recently, the optical centrifuge method was applied to excite molecules to rotational levels with angular momentum of hundreds of \hbar in dense gas samples [5], where collisions play an important role. In this paper we analyze the behavior of a dense gas of unidirectionally spinning molecules after many collisions have occurred. The statistical mechanics and equilibration process of such a system are not trivial, as known for other ensembles in which angular momentum (AM) is a conserved quantity in addition to energy [11, 12]. We show that due to the AM conservation, the collisions in such a gas transform the laser induced molecular rotation into macroscopic vortex flows. The lifetime of the generated vortex motion exceeds the typical collision time by orders of magnitude, and the emerging velocity field eventually converges to a self-similar Taylor vortex [13]. The viscous decay of this whirl can be overcome by repeated laser excitations that produce a continuous stirring effect.

Consider a gas sample excited by laser pulses causing the molecules to rotate, on average, unidirectionally. Our analysis of the subsequent gas dynamics was performed in two steps. First we used a Monte Carlo approach to simulate directly the kinetics of molecular collisions just after the excitation. Then, after the motion had taken a collective character, we used continuum hydrodynamic equations to investigate the gas dynamics and vortex flow evolution.

We analyzed the initial stages of the transformation of the individual molecular rotation into collective gas motion with the help of the Direct Simulation Monte Carlo technique (DSMC [14]). This statistical method is a proven tool for computational molecular dynamics of transitional regimes [15], although the standard DSMC

does not always conserve AM [16, 17]. For this reason, we designed an advanced variant of the DSMC simulation in which angular momentum is strictly conserved. The simulation was run in axisymmetric geometry, and handled collisions using a simple ‘hard dumbbell’ model that treats each ‘molecule’ as a couple of rigidly connected hard spheres [18]. In recent experiments, laser excitation of unidirectional rotation induced an average axial AM in the range of $\langle J_z \rangle \sim 10\hbar - 400\hbar$ [4, 7]. We first simulated a homogeneous sample of such unidirectionally rotating nitrogen molecules put at atmospheric conditions and confined to a smooth cylinder. In order to reduce the statistical fluctuations of the Monte Carlo simulation we averaged the results over multiple runs [19]. Figure 1 shows that within a few collisions ($0.3 - 0.5 ns$ after excitation at our simulation conditions) the energy partition between the translational and rotational degrees of freedom approaches equilibrium. Despite the simplicity of our collision model, it provides the expected energy partition ratio of 3:2 (translation:rotation) typical for diatomic molecules. It takes about ten collision times for the molecules to completely lose memory of the preferred direction of their rotation, supposedly even if the molecules remain in excited rotational states [5].

At longer times, the confined gas rotates rigidly (with tangential velocity linear with the radius) as seen in Fig. 2. This represents a steady state for the motion within a frictionless cylinder, eliminating shear stress. As expected, the results show that the rotation speed is proportional to the total initially induced AM, predicting a steady macroscopic gas rotation frequency of $\sim 10^4 Hz$ for average initial unidirectional rotation of $\langle J_z \rangle \sim 100\hbar$ at atmospheric conditions within a $10 \mu m$ diameter capillary.

At the next stage we analyzed the formation of an unconfined vortex. For this we considered excitation by an axisymmetric laser beam with a Gaussian radial profile. Our study showed that with time, a circular flow develops around the beam’s axis. We examined the spatial and temporal development of the circular flow structure by first running the DSMC simulation for the non-uniform initial rotational excitation. We sampled the results after thermalization, and used continuum gas-dynamic anal-

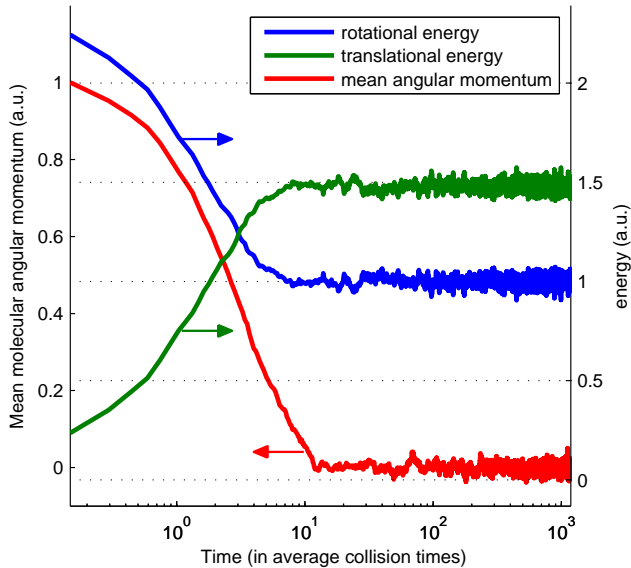


Figure 1. (Color online.) Mean translational energy, rotational energy and molecular axial rotational angular momentum evolution. Initially all the molecules were unidirectionally rotating. The DSMC results show that the final translational:rotational energy ratio reaches 3:2 (green:blue curves, right axis) within about 5 collision times. The average axial component of the molecular AM approaches zero at about 10 collisions, showing that there is no longer a preferred rotation direction. Time axis is logarithmic in units of average collision time ($\sim 10^{-10}$ s).

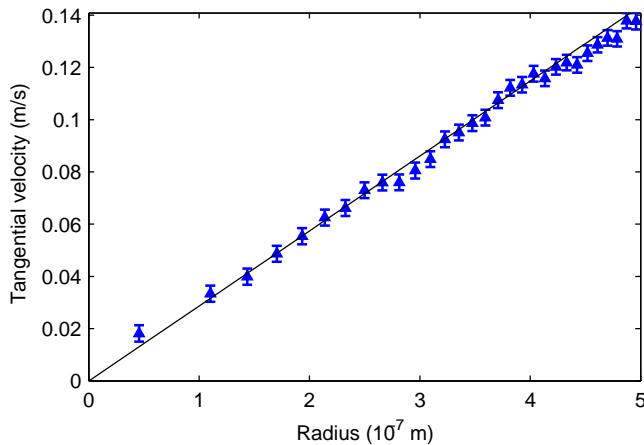


Figure 2. (Color online.) Tangential velocity profile of the gas, which exhibits rigid-body-like rotation. The data are averaged over multiple DSMC runs, covering a time range of $t = 10^{-9} - 2 \cdot 10^{-7}$ s. In this simulation, all the molecules initially rotate with AM of $\langle J_z \rangle \sim 10\hbar$. The bars indicate the statistical error of our procedure. The solid line is a linear fit with $R^2 \sim 0.99$.

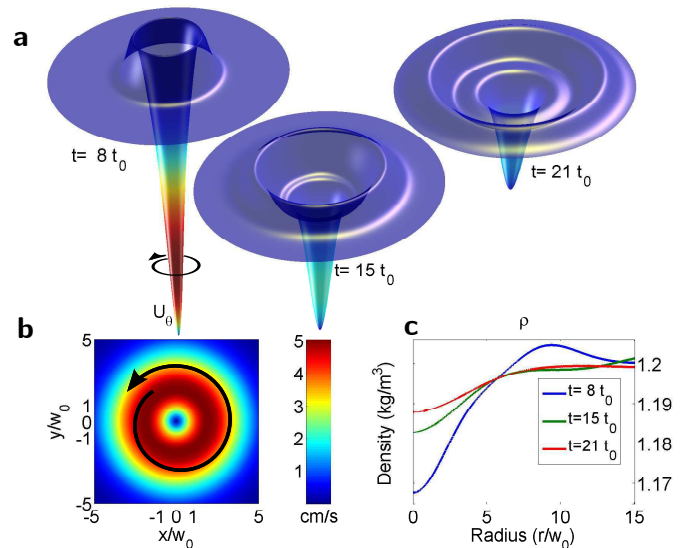


Figure 3. (Color online.) (a) Spatial dependence of the gas density and the tangential velocity of the unidirectional rotation at different times. The time (from left to right) is $8t_0$, $15t_0$ and $21t_0$ after the simulation start (t_0 is the typical vortex timescale, see Eq. (3)). The emerging acoustic wave is clearly visible, and the lower density core can also be noticed. The color coding represents the tangential velocity value, also shown in (b) in the plane perpendicular to the laser beam at $t = 8t_0$. (c) Density radial profile at the same times. The spatial coordinates throughout are in units of w_0 , the radius of the beam's waist.

ysis to unfold the subsequent gas behavior. The gas-dynamic equations we used relate to the mass, energy and momentum conservation in a compressible gas [20]. In order to better account for compressibility we added bulk viscosity [21] terms to the equations, and the ideal gas equation of state concluded the equation set. We used an axially symmetric finite-difference time-domain numerical scheme to solve the problem, with initial conditions based on the DSMC results. The full analysis of the numerical solution will be discussed elsewhere, here we report some of our observations.

Since the laser injects energy to the molecules by rotating them, the gas at the beam's focus is heated following the laser excitation. The subsequent gas expansion creates a density crest, clearly visible on Fig. 3a, that propagates outwards at about the speed of sound.

The radial profile of the directed tangential velocity shows formation of a rigidly rotating core at the laser beam's focal spot. The profile exhibits a diffusion-like behavior in the radial direction. This phenomenon is attributed to the viscosity and is consistent with the notion of 'vorticity diffusion' [22]. After the emerging acoustic wave had left the core, naturally also the temperature spreads diffusively, and so do the other thermodynamic and flow variables (cf. the density plot in Fig. 3c).

At that post-acoustic stage the radial profiles of the

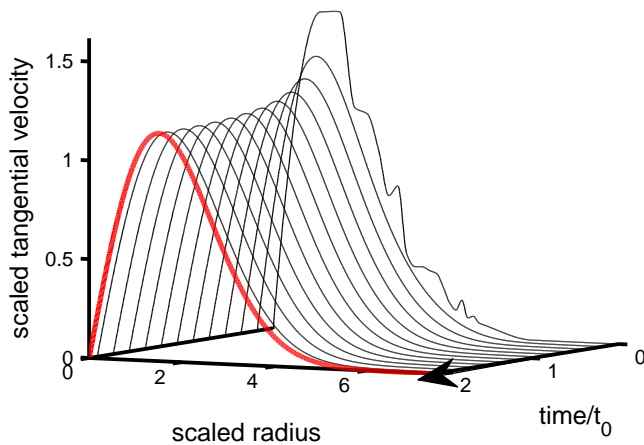


Figure 4. (Color online.) Scaled tangential velocity radial profile at different times. The tangential velocity U_θ is scaled as $U_\theta t^{3/2} \cdot \mathcal{H}^{-1} / [w_0 t_0^{1/2}]$, the radius r is scaled as $rt^{-1/2} / [w_0 t_0^{-1/2}]$. The plot shows a fast convergence to a self-similar Taylor vortex profile (shaded curve, red online) given by Eqs. (2),(3). The time t was offset by a vortex ‘age’ [13] of $0.9 t_0$ to produce the best fit.

velocity, density, pressure and temperature at different times seem to be self-similar. This can be illustrated by examination of the momentum conservation equation (tangential component):

$$\rho \left(\frac{\partial U_\theta}{\partial t} + U_r \frac{\partial U_\theta}{\partial r} + \frac{U_r U_\theta}{r} \right) = \mu \frac{\partial}{\partial r} \left(\frac{1}{r} \frac{\partial}{\partial r} (r U_\theta) \right) \quad , \quad (1)$$

where ρ , U_θ , U_r , μ , r and t are the density, tangential and radial velocity, viscosity, radius and time, respectively. The velocities (e. g., in Fig. 3b) are small compared to the typical velocity ($V_0 = \mu / \rho w_0 \sim 100 \text{ m/s}$, w_0 being the inducing laser beam’s waist radius). We may thus neglect the second order velocity terms in Eq. (1). The relative density variations also shown in Fig. 3c are less than 10%, and by taking a nearly constant viscosity, Eq. (1) reduces to a diffusion equation, with a ‘diffusion coefficient’ proportional to the kinematic viscosity $\nu = \mu / \rho$ [23]. Following that insight, we found self-similar fits to the radial profiles of the gas parameters (after the acoustic wave has left the core). Specifically for the tangential velocity, Fig. 4 shows that the scaled calculated profiles converge with time to the Taylor vortex form [13, 24]:

$$U_\theta(r, t) = \mathcal{H} \frac{w_0}{t_0} \left(\frac{t}{t_0} \right)^{-2} 2\pi \left(\frac{r}{w_0} \right) e^{-\frac{(r/w_0)^2}{(t/t_0)}} \quad , \quad (2)$$

where the length scale w_0 is the radius of the waist of the laser beam, and the typical vortex lifetime is determined by t_0 . The dimensionless parameter \mathcal{H} depends on the average induced AM, and characterizes the number of turnovers the core makes before the vortex’ viscous decay. The parameters t_0 and \mathcal{H} are defined as

$$t_0 = \frac{w_0^2}{4\nu}, \quad \mathcal{H} = \frac{\langle J_z \rangle}{8\pi m_{mol} \cdot \nu} \quad , \quad (3)$$

where $\langle J_z \rangle$ and m_{mol} are the average AM of the molecules excited by the laser and the mass of the individual molecules, respectively.

It follows from Eq. (2) that the rigid core of the vortex rotates at a frequency that drops with time as t^{-2} , while the typical core size grows as $t^{1/2}$. For a tightly focused laser beam ($w_0 \sim 1 \mu\text{m}$) that excites nitrogen molecules at atmospheric conditions to $\langle J_z \rangle \sim 100\hbar$, the vortex parameters are $\mathcal{H} \sim 10^{-2}$, $t_0 \sim 10^{-8} \text{ s}$. In this case a substantial initial rotation frequency of $\sim 10^5 \text{ Hz}$ may be achieved.

Consider now the motion of gas parcels as the vortex develops and decays. We calculated the parcels’ trajectories both numerically and analytically with the help of Eq. (2), mapping each point to its location after the vortex had died. The jolt imparted by the laser excitation results in a finite angular displacement of the gas parcel. By repeating the excitation again and again the angular displacement accumulates, rotating parcels around the beam’s axis as a ‘micro-torque-gun’, producing a motion similar to that of a ticking watch dial. At a pulse repetition rate of 1 kHz , the time interval between pulses is long enough for diffusion to wipe the temperature and density inhomogeneities and any radial displacement, even on millimeter-scale. Thus, in the micron-size waist of the laser beam only the azimuthal displacement grows from jolt to jolt. Figure 5 and the Supplementary Video [25] visualize the angular displacement after many iterations. This angular displacement pattern can be observed by following the motion of micron-sized particles suspended in the whirling gas.

To conclude, we showed that laser pulses that induce unidirectional rotation of individual gas-molecules produce a long-lasting macroscopic rotation of the gas. In a frictionless cylinder the gas reaches a steady rigid-body-like rotation. In free space a self-similar vortex forms and lasts significantly longer than both the pulse duration and the typical collision time. We also demonstrated that a repeated laser excitation can stir the gas in a pounding ‘torque-gun’ motion accumulating to large angular displacement. The 100 kHz rotational motion of the gas vortex may be detected with the help of the rotational Doppler effect [26–28] or by usage of structured light spectroscopy [29]. According to our estimations the predicted collective spiraling motion is also observable by monitoring the motion of particles suspended in the gas. Finally, we emphasize that the appearance of the gas vortex is a direct manifestation of angular momentum conservation. In a sense, our laser-induced effect presents a table-top analogue to the formation of tropospheric cyclones, in which global rotational structures appear due to the inverse cascade scale-up starting from the motion

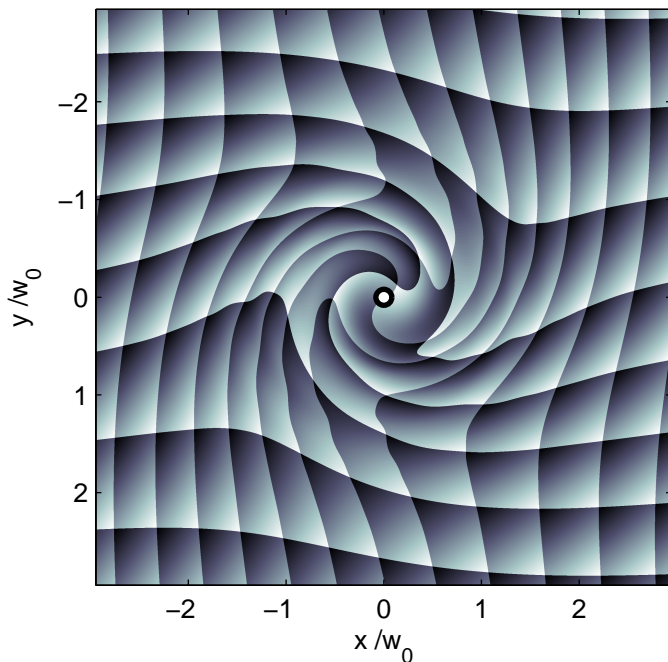


Figure 5. Accumulated displacement deformation of a virtual rectangular mesh after 6,000 pulse sets, for $\mathcal{H} \sim 10^{-4}$. The angular displacement is clearly visible around the center (circle marker). The coordinates are in the plane perpendicular to the laser beam, in units of the laser beam's waist radius w_0 .

of turbulent eddies [30, 31].

Financial support for this research from the Israel Science Foundation is gratefully acknowledged. This research is made possible in part by the historic generosity of the Harold Perlman Family. The authors thank Dennis C. Rapaport, Robert J. Gordon and Rigoberto Hernandez for helpful discussions.

* uri.steinitz@weizmann.ac.il

- [1] H. Stapelfeldt and T. Seideman, *Rev. Mod. Phys.* **75**, 543 (2003).
- [2] B. Friedrich and D. Herschbach, *Phys. Rev. Lett.* **74**, 4623 (1995); *J. Chem. Phys.* **111**, 6157 (1999).
- [3] J. Karczmarek, J. Wright, P. Corkum, and M. Ivanov, *Phys. Rev. Lett.* **82**, 3420 (1999).
- [4] D. M. Villeneuve, S. A. Aseyev, P. Dietrich, M. Spanner, M. Y. Ivanov, and P. B. Corkum, *Phys. Rev. Lett.* **85**, 542 (2000).
- [5] L. Yuan, S. W. Teitelbaum, A. Robinson, and A. S. Mullin, *Proc. Natl. Acad. Sci. USA* **108**, 6872 (2011).
- [6] S. Fleischer, Y. Khodorkovsky, Y. Prior, and I. S. Averbukh, *New J. Phys.* **11**, 15 (2009).
- [7] K. Kitano, H. Hasegawa, and Y. Ohshima, *Phys. Rev. Lett.* **103**, 223002 (2009).
- [8] S. Zhdanovich, A. A. Milner, C. Bloomquist, J. Floß, I. S. Averbukh, J. W. Hepburn, and V. Milner, *Phys. Rev. Lett.* **107**, 243004 (2011).
- [9] J. P. Cryan, J. M. Glowina, D. W. Broege, Y. Ma, and P. H. Bucksbaum, *Phys. Rev. X* **1**, 011002 (2011).
- [10] M. Lapert, S. Guérin, and D. Sugny, *Phys. Rev. A* **83**, 013403 (2011).
- [11] F. Román, A. González, J. White, and S. Velasco, *J. Chem. Phys.* **118**, 7930 (2003).
- [12] M. Uranagase, *Phys. Rev. E* **76**, 061111 (2007).
- [13] G. I. Taylor, *On the dissipation of eddies*, Reports and Memoranda no. 598 (Brit. Advis. Comm. Aeronaut., 1918).
- [14] G. A. Bird, *Molecular Gas Dynamics and the Direct Simulation of Gas Flows*, Oxford engineering science series (Clarendon Press ;Oxford University Press, Oxford, New York, 1994).
- [15] P. Prasanth and J. Kakkassery, *Fluid Dyn. Res.* **40**, 233 (2008).
- [16] K. Nanbu, Y. Watanabe, and S. Igarashi, *J. Phys. Soc. Jpn.* **57**, 2877 (1988).
- [17] G. A. Bird, *Phys. Fluids* **30**, 364 (1987).
- [18] M. P. Allen, D. Frenkel, and J. Talbot, *Comp. Phys. Rep.* **9**, 301 (1989).
- [19] N. Hadjiconstantinou, A. Garcia, M. Bazant, and G. He, *J. Comp. Phys.* **187**, 274 (2003).
- [20] T. Colonius, S. K. Lele, and P. Moin, *J. Fluid Mech.* **230**, 45 (1991).
- [21] M. Gad-el Hak, *J. Fluids Eng.* **117**, 3 (1995).
- [22] S. I. Green, *Fluid Vortices*, Fluid Mechanics and its Applications, Vol. 30 (Kluwer Academic Publishers, Dordrecht ; Boston, 1995).
- [23] F. Grasso and S. Pirozzoli, *Phys. Fluids* **11**, 1636 (1999).
- [24] A. de Neufville, in *Fifth Midwestern Conference on Fluid Mechanics* (University of Michigan, 1957) pp. 365–375.
- [25] See Supplemental Material at [URL will be inserted by publisher] for a video showing the accumulated displacement deformation of a virtual rectangular mesh as multiple vortex laser excitation are made. It spans over 15,000 iterations, exhibiting a substantial angular displacement. The coordinates are in units of the radius of the laser beam waist w_0 , the vortex parameter is $\mathcal{H} \sim 10^{-4}$.
- [26] B. A. Garetz, *J. Opt. Soc. Am.* **71**, 609 (1981).
- [27] L. Allen, M. Babiker, and W. L. Power, *Opt. Commun.* **112**, 141 (1994).
- [28] S. Barreiro, J. W. R. Tabosa, H. Failache, and A. Lezama, *Phys. Rev. Lett.* **97**, 113601 (2006).
- [29] D. L. Andrews, *Structured Light and its Applications : an Introduction to Phase-Structured Beams and Nanoscale Optical Forces* (Academic Press, Amsterdam ; Boston, 2008).
- [30] E. Fedorovich, R. Rotunno, B. Stevens, and D. Lilly, *Atmospheric Turbulence and Mesoscale Meteorology*, edited by E. Fedorovich, R. Rotunno, and B. Stevens (Cambridge University Press, Cambridge, 2004).
- [31] P. Tabeling, *Phys. Rep.* **362**, 1 (2002).